1-1-2015

3D printed terahertz diffraction gratings and lenses

A D. Squires
University of Wollongong, ads786@uowmail.edu.au

E Constable
University of Wollongong, evanc@uow.edu.au

R A. Lewis
University of Wollongong, roger@uow.edu.au

3D printed terahertz diffraction gratings and lenses

Abstract

3D printing opens up an inexpensive, rapid, and versatile path to the fabrication of optical elements suited to the terahertz regime. The transmission of the plastics used in 3D printers, while generally decreasing with frequency, is usable over the range 0.1-2 THz. We have designed, fabricated, and tested regular and blazed gratings and aspherical lenses for operation at terahertz frequencies. We find that the measured performance matches our theoretical predictions.

Disciplines

Engineering | Science and Technology Studies

Publication Details

Squires, A. D., Constable, E. & Lewis, R. A. (2015). 3D printed terahertz diffraction gratings and lenses. Journal of Infrared, Millimeter, and Terahertz Waves, 36 (1), 72-80.

Journal of Infrared, Millimeter, and Terahertz Waves manuscript No.
(will be inserted by the editor)

3D printed terahertz diffraction gratings and lenses

A. D. Squires · E. Constable ·
R. A. Lewis

Received: 19 September 2014 / Revised: 30 September 2014 / Accepted: 25 October 2014

Abstract 3D printing opens up an inexpensive, rapid, and versatile path to the fabrication of optical elements suited to the terahertz regime. The transmission of the plastics used in 3D printers, while generally decreasing with frequency, is usable over the range 0.1–2 THz. We have designed, fabricated, and tested regular and blazed gratings and aspherical lenses for operation at terahertz frequencies. We find that the measured performance matches our theoretical predictions.

Keywords Terahertz · THz · 3D printing · additive fabrication · diffraction · blazed · grating · aspherical · lens · poly(lactic acid) · polyactide · VisiJet

1 Introduction

New methods are revolutionizing manufacturing. Items which were traditionally made by "subtractive" methods, for example, removing the unwanted material on a lathe with a tool to give the final turned product, are now being made by "additive" methods, that is, by building up the final product layer by layer. Inexpensive, compact, computer-controlled 3D printers are in the vanguard of this innovation.

Terahertz technology stands to benefit from the additive manufacturing revolution. Typical terahertz optical elements include lenses and diffraction gratings [1]. Conventionally, optical elements have been made by subtractive methods, such as machining lenses on a lathe [2], or cutting grooves in a

A. D. Squires · E. Constable · R. A. Lewis
Institute for Superconducting and Electronic Materials
and
School of Physics
University of Wollongong, Wollongong, NSW 2522, Australia
Tel.: +61-2-4221-3518
Fax: +61-2-4221-5944
E-mail: ads786@uowmail.edu.au

substrate to form a diffraction grating [3,4]. An alternative manufacturing strategy, well-suited to mass production, is to mold the product in a die of appropriate shape. Both terahertz gratings [5] and terahertz lenses [6,7] have been made by the compression of micropowders. Recently, the possibility has opened up to make terahertz optical elements quickly, cheaply, and with extraordinary control by additive fabrication using 3D printers. Both generic and propriety plastic media are available.

While this paper concentrates on 3D printed plastic gratings and lenses, we note that other optical elements have been reported based on plastic and are also amenable to production by 3D printing. Such optical elements as dielectric fibers (waveguides)[8] and prisms [9] have been made from polypropylene. Even terahertz mirrors [10,11] now include polypropylene in their design [12].

2 Theory

2.1 Regular grating

The geometry of the regular grating [13] is shown in Fig. 1.

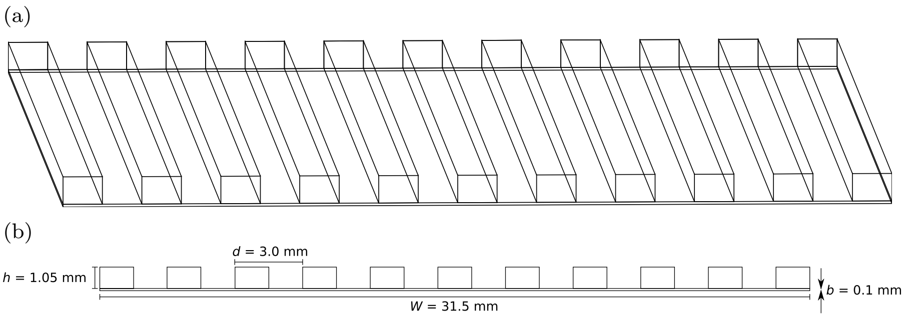

Fig. 1 Regular grating. The period of the structure is $d = 3$ mm. The height of each bar is $h = 1.05$ mm. The structure is supported by a thin base of thickness $b = 0.1$ mm. The overall width is $W = 31.5$ mm (10.5 periods) and the overall length is $L = 20$ mm. (a) Perspective view. (b) Side view.

The diffraction gratings were designed to operate at a frequency, f, of 0.2 THz, corresponding to a wavelength, λ, of 1.5 mm. The material chosen was poly(lactic acid), also known as polyactide (PLA). Using terahertz time-domain spectroscopy (employing a Z-2 spectrometer from Z-omega), we determined the refractive index of PLA at $f = 0.2$ THz to be $n = 1.715$.

To obtain intensity in the first-order diffraction peak a period of $d = 2\lambda = 3$ mm was chosen. To suppress the even orders of diffraction, the height of the rectangular bars was set at $h = \lambda/2(n-1) = 1.05$ mm.

The diffraction grating structure was supported on a PLA base of $b = 0.1$ mm. The overall width, W, of the structure was 10.5 periods, or 31.5 mm; the overall length, L, was 20 mm.

Scalar diffraction theory gives the transmission of the regular grating to be [14]:

$$f(x) = \left\{ \left[\mathrm{rect}(\frac{2x}{d}) \otimes \delta(x) \right] + \left[\mathrm{rect}(\frac{2x}{d}) \otimes \delta(x - d/2) \right] \exp(i\phi) \right\} \otimes \mathrm{comb}(\frac{x}{d}). \tag{1}$$

Here x is the distance from the origin along the grating (the first "step" in the grating is centered at $x = 0$) and ϕ is the phase difference. The phase difference is given by $\phi = (2\pi h/\lambda)(n - 1)$.

2.2 Blazed grating

The geometry of the blazed grating is shown in Fig. 2.

(a)

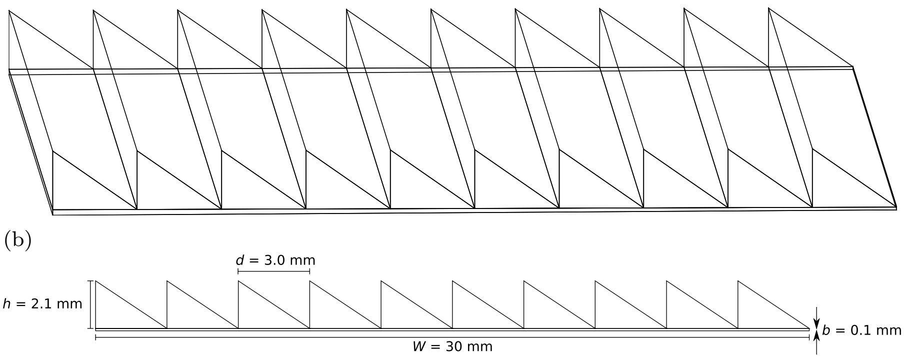

Fig. 2 Blazed grating. The period of the structure is $d = 3$ mm. The height of each wedge is $h = 2.1$ mm. The structure is supported by a thin base of thickness $b = 0.1$ mm. The overall width is $W = 30$ mm (10 periods) and the overall length is $L = 20$ mm. (a) Perspective view. (b) Side view.

As with the regular grating, to obtain intensity in the first-order diffraction peak, a period of $d = 2\lambda = 3$ mm was chosen for the blazed grating. In the case of the blazed grating, to suppress the even orders of diffraction, the height of the grating was set at $h = \lambda/(n - 1) = 2.1$ mm, twice as high as the regular grating. Again as with the regular grating, the blazed grating structure was built on a base of $b = 0.1$ mm of PLA. The overall width, W, was 10 periods (30 mm) and the overall length, L, was 20 mm.

The blazed grating equation is:

$$f(x) = \mathrm{comb}(\frac{x}{d}) \otimes \mathrm{rect}(\frac{x}{d}) \exp(\frac{i\phi x}{d}). \tag{2}$$

As before, x is the distance from the origin along the grating, d is the period of the grating, and ϕ is the phase difference, again given by $(2\pi h/\lambda)(n - 1)$. The blaze has a gradient of ϕ/d.

3 Experiment

The gratings were produced using an Ultimaker Original 3D printer utilizing fused filament fabrication (FFF; equivalent to FDM) and a nozzle diameter of 0.4 mm. This setup prints with 2.85 mm PLA or ABS filament. The gratings were made with the following specifications: layer height 0.01 mm, shell thickness 0.1 mm, print speed 50 mm/s, and print temperature 220 degrees Celsius. To ensure a smoother finish, the lenses were produced by Multi-Jet-Modelling using a ProJet HD3500 plus, using the proprietary plastic sold as "Visijet" and with a print temperature of 18–28 degrees Celsius.

Both the gratings and lenses are mechanically robust. Although the base of the gratings is thin (0.1 mm), the gratings do not easily bend or break and are substantially stronger than other commonly-used optical components such as beamsplitters and pellicles. Bijarimi *et al.* have given some mechanical properties of PLA as breaking stress 69.9 MPa, Young's modulus 1968 MPa, and flexural modulus 3536 MPa [15]. For VisiJet, the tensile strength is specified by the manufacturer to be 42.4 MPa and the flexural strength to be 49 MPa.

The experimental setup is shown in Fig. 3. The THz source consists of a continuous-wave quasi-monochromatic photomixer system. The photomixer is pumped by two fiber-coupled frequency-offset near-infrared (NIR) diode lasers (Toptica DL-100, $\lambda_0 = 853 \pm 3$ nm). The laser frequency difference determines the THz frequency and this is measured by a fiber-coupled optical spectrum analyser (OSA) monitoring the laser modes. Adjusting the frequency difference of the lasers allows for THz tuning from 0.1–1.0 THz. For the purposes of this experiment, the frequency of the THz source was fixed at 0.2 THz. The photomixer bias is modulated from 0–20 V at 183 Hz for lock-in detection using a liquid-He–cooled Si bolometer.

Both the lens and the diffraction-grating measurements are performed in transmission geometry. For the lenses, the focal length was measured by moving the lens along the optic axis relative to the detector, along the collimated THz beam. For the gratings, the THz beam is first collimated and then focused onto the grating using two off-axis gold-plated parabolic mirrors. Keeping a fixed distance of 100 mm from the diffraction grating, the bolometer position is rotated through an angle θ relative to the grating normal. Measurements of the transmitted intensity were taken at angular increments of 1 degree with a 1 second integration time.

4 Results

4.1 Transmission in the THz regime

The absorption coefficients of PLA and VisiJet are shown in Fig. 4. In common with many organic materials, the transmission is very good in the sub-THz range, then decreases with frequency. There is no clear cut-off in the frequency below which the materials may be used. If 0.1 transmission at 1 mm thickness is

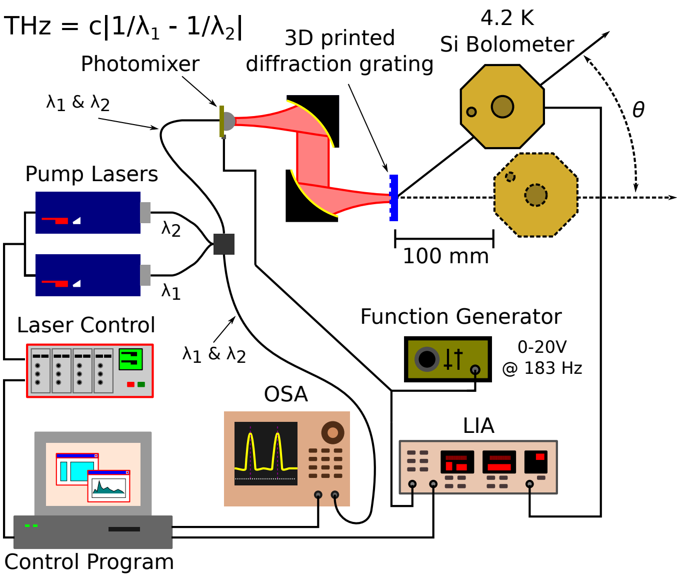

Fig. 3 Experimental apparatus.

taken as the criterion, both materials are useful to about 0.7 THz. Other plastics have superior transmission in this range. See, for example, Ganichev and Prettl, Fig. 1.29 for black polyethylene, high-density polyethylene, polystyrene, polypropylene and polythene, and Fig. 1.30 for TPX, teflon, di-acetil cellulose, tri-acetil cellulose, mylar, and pertinax [16].

The results presented hereafter are all at frequency $f = 0.2$ THz. We designed the gratings as phase gratings but, in view of the non-negligible absorption, they will behave to some extent as amplitude gratings as well.

4.2 Gratings

The data pertaining to the regular grating appear in Fig. 5. Also shown in the figure is the expected behavior as calculated from Eq. (1). It is seen that good agreement is obtained. In theory, there should be no transmission in the straight-through direction ($\theta = 0$), and equal peaks at $\theta = \pm 30$ degrees. While there is some leakage through the fabricated grating at $\theta = 0$, the equal peaks at $\theta = \pm 30$ degrees are apparent in the experimental data. The side lobes that are evident in the theory are hinted at in the experimental data by shoulders on the main peaks but the solid angle subtended by the detector is too large for these to be clearly resolved in the present experimental setup.

The data pertaining to the blazed grating appear in Fig. 6. Also shown in the figure is the expected behavior as calculated from Eq. (2). It is seen that good agreement is obtained. It is expected that diffraction peaks will occur at $\theta = -30$ degrees, $\theta = 0$ degrees, and $\theta = +30$ degrees, which is borne out by

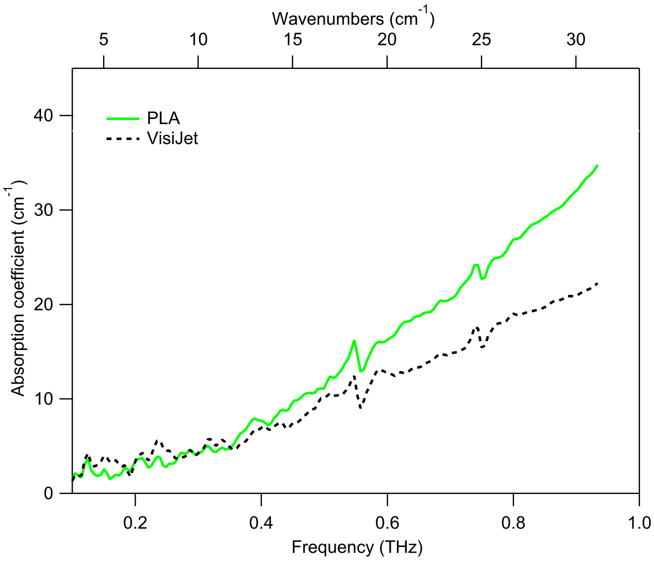

Fig. 4 Absorption coefficient of PLA (full, green line) and VisiJet (dashed, black line) plastic printing materials.

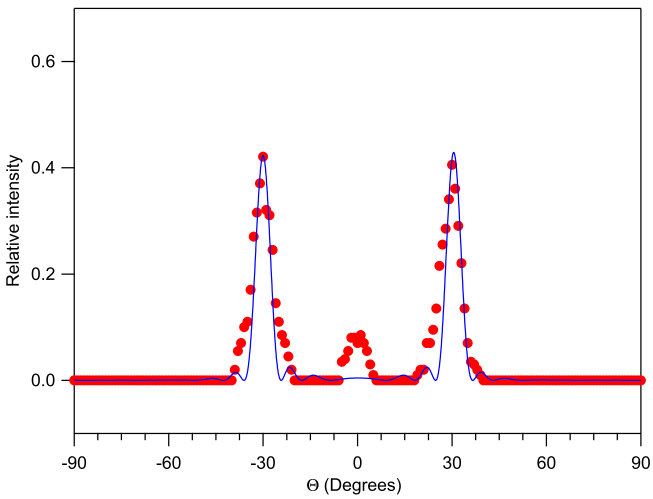

Fig. 5 Regular grating. Full circles—experiment. Full line—theory. The intensity is relative to the intensity when there is no grating in the beam.

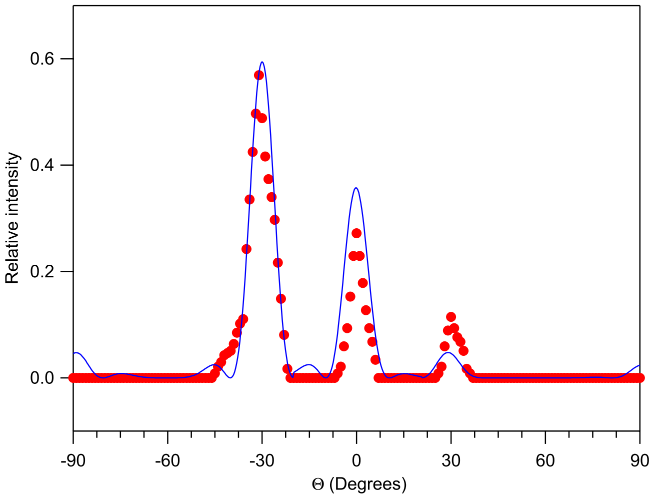

Fig. 6 Blazed grating. Full circles—experiment. Full line—theory. The intensity is relative to the intensity when there is no grating in the beam.

Table 1 Key characteristics of 3D printed gratings—theory and experiment

Order		$m = 0$	$m = +1$	$m = -1$
Regular grating				
Position (degrees)	—theory	0	+30	−30
	—experiment	0 ± 0.5	$+30 \pm 0.1$	-30 ± 0.1
Intensity (%)	—theory	0	46	46
	—experiment	12 ± 1	45 ± 1	43 ± 1
Blazed grating				
Position (degrees)	—theory	0	+30	−30
	—experiment	0 ± 0.1	$+30 \pm 0.1$	-30 ± 0.1
Intensity (%)	—theory	35	60	5
	—experiment	28 ± 1	60 ± 1	12 ± 1

experiment. The ratios of intensity are measured to be $60 \pm 1 : 28 \pm 1 : 12 \pm 1$, again close to the values as expected theoretically.

A numerical comparison between the experiment and theory is given in Table 1 for both the regular and the blazed grating.

4.3 Lenses

Preliminary measurements have also been made on 3D-printed lenses. The three lens designs chosen are illustrated in Fig. 7. They are symmetric, elliptical-aspheric, and planar-hyperbolic [2].

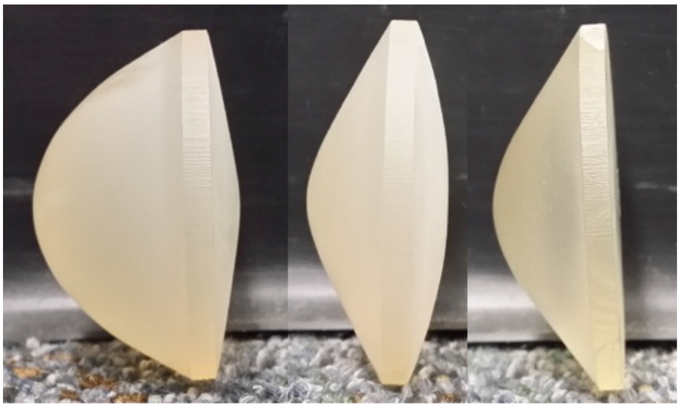

Fig. 7 Aspherical lenses fabricated by 3D printing (a) Symmetric, (b) Elliptical-aspheric, (c) Planar-hyperbolic.

For each of the fabricated lenses, the focal length was measured to be 35 ± 2 mm. This is consistent with the calculated focal lengths, taking into account the cone angle and radial distance from the optical axis [2]. However, the absorption in these relatively thick optical elements has prevented more thorough optical characterization. Thinner lens designs and equivalent Fresnel lenses are the goal of ongoing work.

5 Conclusion

In conclusion, we have demonstrated that 3D printing techniques are effective for the fabrication of complex optical structures in the THz domain. This is a significant result as 3D printing offers a method for low cost, versatile, and fast fabrication. A blazed and regular grating design optimized for diffraction at 0.2 THz were considered with the diffraction patterns measured at a distance of 100 mm. The results, when compared to theoretically determined angular dependence, showed good agreement. Often the limitations of resolution and usable materials in 3D printing are a disadvantage for a wide range of fabrication applications. Our results establish that at THz frequencies the optical properties of the printable materials are favorable, at least for thin layers at low frequencies, and that the printable resolution is fine enough for the wavelengths of interest.

Acknowledgements This work was supported by the Australian Research Council and by the University of Wollongong. We thank EMCORE Corporation (J. Demers) for the provision of the excellent photomixer used in the experiments reported here. We are grateful to E. Li for assistance with the optical alignment of the apparatus.

References

1. R.A. Lewis, *Terahertz Physics* (Cambridge: Cambridge University Press, 2012)
2. L. Lo, R. Leonhardt, Optics Express **16**(20), 15991 (2008)
3. J.L. Coutaz, F. Garet, E. Bonnet, A.V. Tishchenko, O. Parriaux, M. Nazarov, Acta Physica Polonica **107**(1) (2005)
4. N.S. Stoyanov, T. Feurer, D.W. Ward, K.A. Nelson, Appl. Phys. Lett. **82**(5), 674 (2003)
5. S.F. Busch, N. Born, M. Koch, B. Fischer, Journal of Infrared, Millimeter, and Terahertz Waves **34**(7–8), 413 (2013)
6. B. Scherger, M. Scheller, C. Jansen, M. Koch, K. Wiesauer, Appl. Optics **50**(15), 2256 (2011)
7. B. Scherger, S. Wietzke, M. Scheller, N. Vieweg, M. Wichmann, M. Koch, K. Wiesauer, Journal of Infrared, Millimeter, and Terahertz Waves **32**(7), 943 (2011)
8. C. Jördens, K. Chee, I. Al-Naib, I. Pupeza, S. Peik, G. Wenke, M. Koch, Journal of Infrared, Millimeter, and Terahertz Waves **31**(2), 214 (2010)
9. C. Goy, M. Scheller, B. Scherger, V.P. Wallace, M. Koch, Optics Express **21**(16), 19292 (2013)
10. H.B. Ye, Y.H. Zhang, W.Z. Shen, Thin Solid Films **514**, 310 (2006)
11. M. Tecimer, K. Holldack, L.R. Elias, Phys. Rev. ST Accel. Beams **13**, 030703 (2010)
12. N. Krumbholz, K. Gerlach, F. Rutz, M. Koch, R. Piesiewicz, T. Kürner, D. Mittleman, Appl. Phys. Lett. **88**(20), 202905 (2006)
13. E. Lowan, E.Popov, Optics and Spectroscopy **88**(1), 143 (2000)
14. R. Casini, P.G. Nelson, Journal of the Optical Society of America A **10**, 2179 (2014)
15. M. Bijarimi, S. Ahmad, R. Rasid, in *International Conference on Agriculture, Chemical and Environmental Sciences (ICACES'2012)* (2012), pp. 115–117
16. S.D. Ganichev, W. Prettl, *Intense Terahertz Excitation of Semiconductors* (Oxford: Oxford Science Publications, 2006)